

Imaging of Anal Fistulas: Comparison of Computed Tomographic Fistulography and Magnetic Resonance Imaging

Changhu Liang, MD¹, Yongchao Lu, MD², Bin Zhao, MD¹, Yinglin Du, BA³, Cuiyan Wang, MD¹, Wanli Jiang, MSc⁴

¹Shandong Medical Imaging Research Institute, Shandong University, Jinan 250021, China; ²Traditional Chinese Medicine Department, Provincial Hospital Affiliated to Shandong University, Jinan 250021, China; ³Shandong Provincial Center for Disease Control and Prevention, Public Health Institute, Jinan 250014, China; ⁴Department of Radiology, Taishan Medical University, Taian 271000, China

The primary importance of magnetic resonance (MR) imaging in evaluating anal fistulas lies in its ability to demonstrate hidden areas of sepsis and secondary extensions in patients with fistula in ano. MR imaging is relatively expensive, so there are many healthcare systems worldwide where access to MR imaging remains restricted. Until recently, computed tomography (CT) has played a limited role in imaging fistula in ano, largely owing to its poor resolution of soft tissue. In this article, the different imaging features of the CT and MRI are compared to demonstrate the relative accuracy of CT fistulography for the preoperative assessment of fistula in ano. CT fistulography and MR imaging have their own advantages for preoperative evaluation of perianal fistula, and can be applied to complement one another when necessary.

Index terms: CT; MR imaging; Fistulography; Perianal fistula

INTRODUCTION

Fistula in ano is a common condition defined by an abnormal perianal track that connects two epithelialized surfaces, usually the anal canal to the perianal skin (1, 2). Some fistulas have a tendency to recur, despite seemingly curative surgery, and recurrence rates may reach 25% (3). Successful surgical management of anal fistulas requires an accurate preoperative assessment of the primary fistula's course and the affected pelvic structures (4).

Received March 8, 2014; accepted after revision September 13, 2014.

Corresponding author: Yongchao Lu, MD, Traditional Chinese Medicine Department, Provincial Hospital Affiliated to Shandong University, No.324, Jingwu Road, Jinan 250021, China.

• Tel: (86531) 85187547 • Fax: (86531) 87938911
• E-mail: yongchaolu123456@163.com

This is an Open Access article distributed under the terms of the Creative Commons Attribution Non-Commercial License (<http://creativecommons.org/licenses/by-nc/3.0>) which permits unrestricted non-commercial use, distribution, and reproduction in any medium, provided the original work is properly cited.

The advantages of magnetic resonance (MR) imaging include multiplanar imaging and a high degree of soft tissue differentiation (5). The primary importance of MR imaging lies in its ability to demonstrate hidden areas of sepsis and secondary extensions (6). MR imaging is relatively expensive, so there are many healthcare systems worldwide, especially in the underdeveloped countries, where access to MR imaging remains restricted. MR imaging does not use ionizing radiation, but rather strong magnetic fields and radio waves. The major drawbacks of routine MR imaging usage are the time and expense of the procedure. The restrictive nature of MR imaging and the long periods of necessary immobility make some patients feel uncomfortable and claustrophobic. Until recently, computed tomography (CT) has played a limited role in imaging fistulas in ano, largely owing to its poor resolution of soft tissue (7). Although the application of volumetric thin-slice CT fistulography or contrast-enhanced scans can bridge the aforementioned issues, researchers have not conducted much research in the field and a clear consensus has yet

Table 1. Suggested Protocol for MR Imaging of Perianal Fistulas

Parameters	Imaging Plane	TR/TE (msec)	FOV (cm)	Section Thickness (mm)	Intersection Gap (mm)	Matrix
T2W FSE	Sagittal	3800/118	26 x 26	3	0.2	512 x 320
T1W FSE	Oblique axial	744/13	30 x 30	5	0.3	320 x 256
T2W FSE	Oblique axial	3600/138	28 x 28	3.5	0.2	512 x 320
FS T1W FSE	Oblique axial	700/18	30 x 30	5.0	0.2	320 x 224
FS T1W FSE	Oblique coronal	750/12	35 x 35	5.0	0.2	512 x 256
LAVA	Oblique axial	3.4/1.4	25 x 25	4	0	320 x 224

Note.— FOV = field of view, FS = fat-suppressed, FSE = fast spin-echo, LAVA = liver acquisition with volume acceleration, T1W = T1-weighted, T2W = T2-weighted, TE = echo time, TR = repetition time

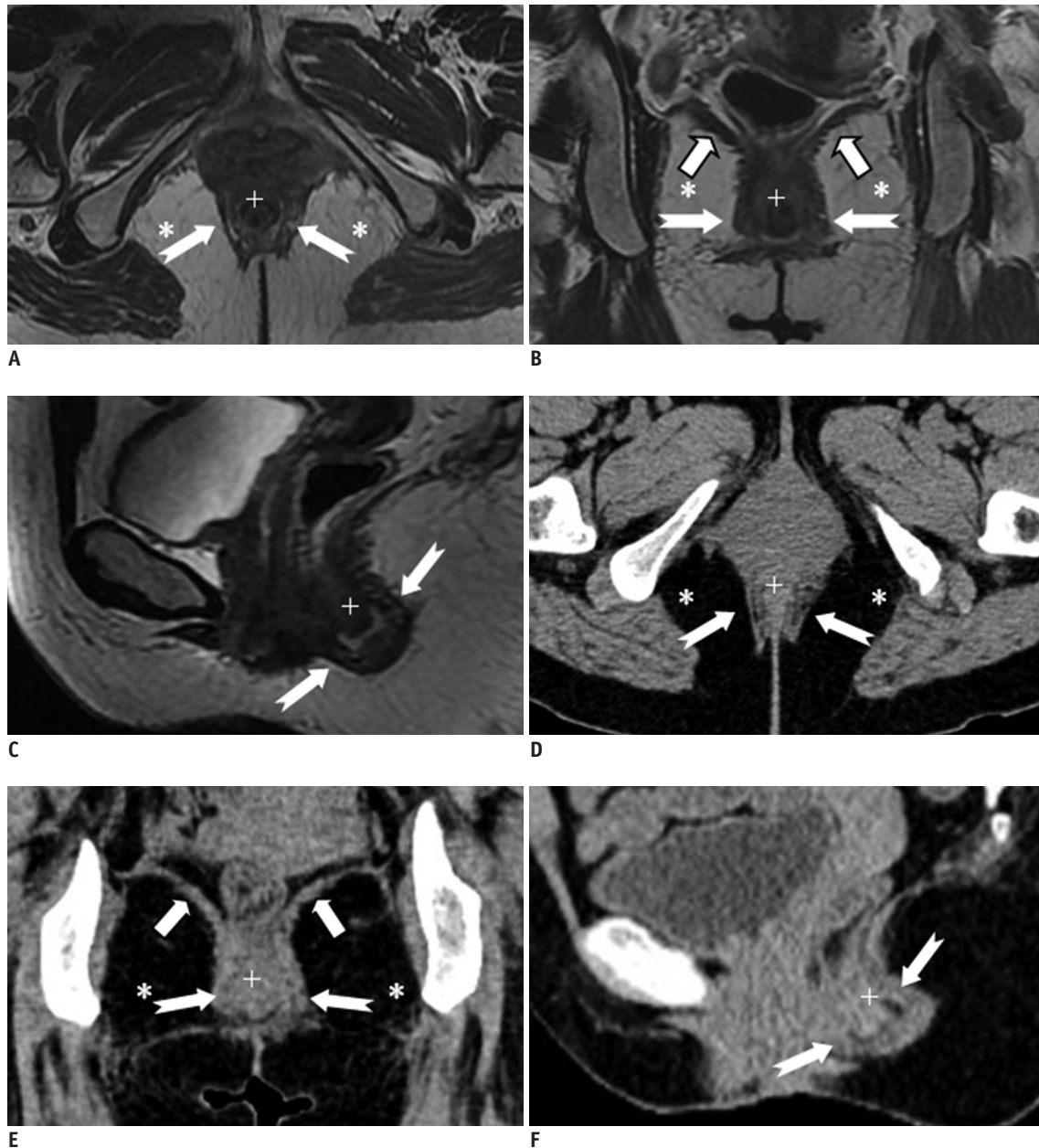


Fig. 1. Normal perianal anatomy of 47-year-old female volunteer imaged with CT and MR imaging.

Anal sphincter complex is seen as two concentric rings. MR imaging: inner (+) internal sphincter and outer external sphincter (white dovetail arrows) appear relatively hypointense on all T2-weighted images without fat suppression (A-C). Levator ani muscle (B, thick arrows) forms superior boundary of fat-containing ischioanal fossa (*) on either side of anal canal. CT (D-F) of inner internal sphincter (+), outer external sphincter (white dovetail arrows), levator ani muscle (E, thick arrows), and fat-containing ischioanal fossa (*).

to appear in the literature.

In order to demonstrate the relative accuracy of CT fistulography for the preoperative assessment of fistula in ano, the different imaging features in CT fistulography and MR imaging were compared side by side.

Techniques and Methods

Anal MR imaging at our institution was performed on a Signa EXCITE 3.0-T scanner (GE Healthcare, Milwaukee, WI,

USA) by using a routine protocol for pelvic examinations containing T1 and T2 three-planer views (axial, coronal and sagittal planes), with the application of a contrast medium (Table 1). No special bowel preparation was used.

The CT perianal region scan was performed on a second-generation dual-source scanner (Somatom Definition Flash, Siemens Medical Solutions, Erlangen, Germany) for low doses of radiation with following parameters: kVp, 120; mAs, 100; collimation, 128 x 0.6 mm with z-flying focal spot; 4D dose modulation (Care Dose 4D); pitch, 1.2;



Fig. 2. Normal perianal anatomy of 45-year-old male volunteer imaged with CT and MR imaging.

MR imaging (T2-weighted without fat suppression images; A-C) and CT (D-F): anal sphincter complex is seen as two concentric rings. Inner internal sphincter (+), outer external sphincter (white or black dovetail arrows), levator ani muscle (thick arrows), fat containing ischioanal fossa (*).

Imaging of Anal Fistulas

rotation time, 0.5 second. Two separate CT scans were performed in all patients. The aims of the first intravenous contrast scan were as follows: 1) to confirm the key factor related to perianal fistulas, as various conditions associated with perianal fistulas including Crohn's disease, previous surgery, tuberculosis, pelvic infection, or pelvic malignancy were easily scrutinized; and 2) to ascertain the feasibility

of fistulography. The second scan with fistulography was performed about half an hour after the first scan.

The patient was placed in prone position. Anal gas injection was then performed in order to discover the internal fistula opening. Adequate colonic or rectal distension is crucial for a full display of the internal opening. Prior to scanning, an enema tip was inserted into

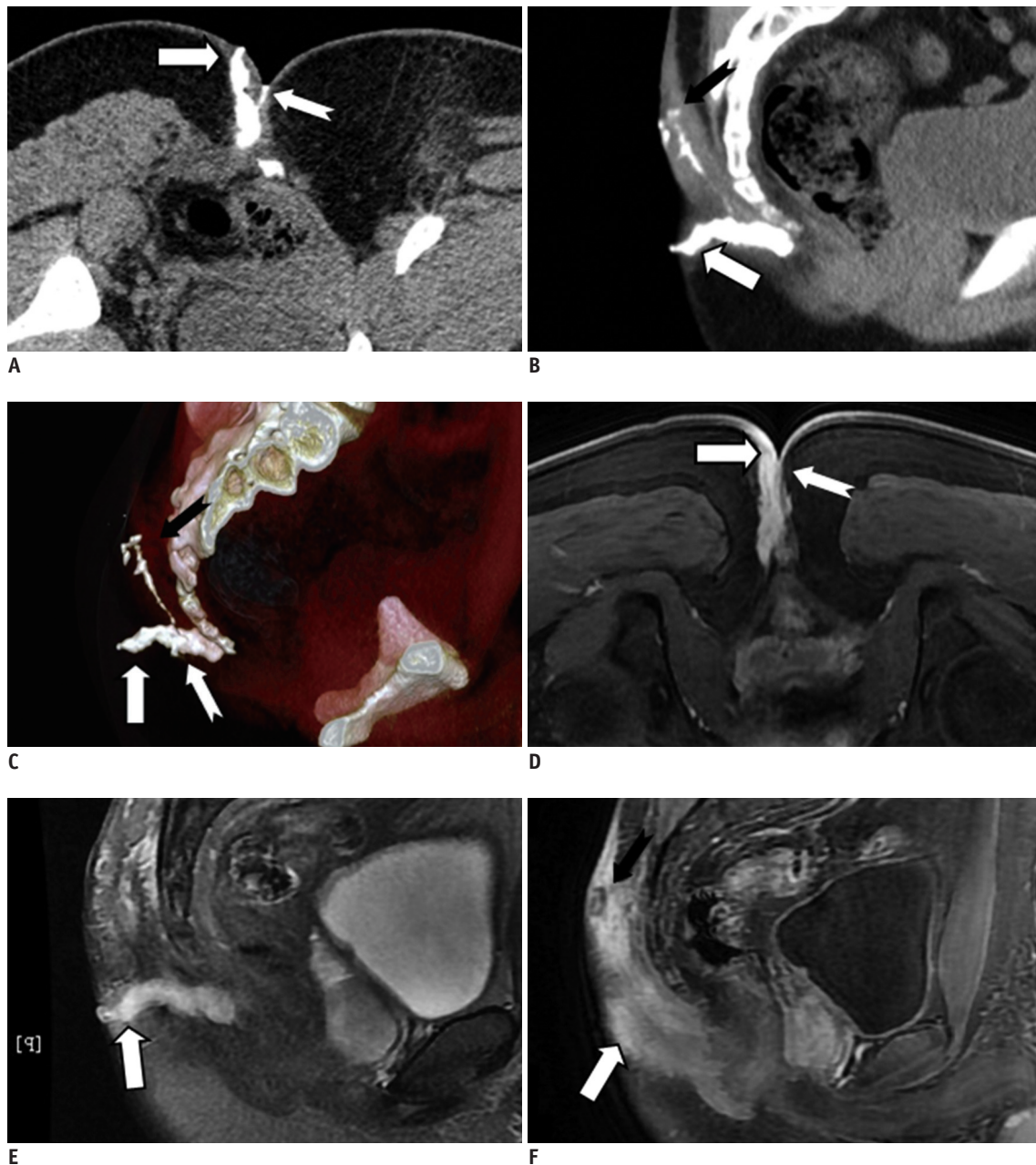


Fig. 3. 21-year-old male with perianal complex fistulas.

CT fistulography images clearly show complex perianal fistula tracts in subcutaneous shallow area, in rear of coccyx. Three anomalous fistula tracts with external opening were successfully identified. Extent of disease and complicated spatial information are better seen on volume rendering image. Minute fistula was not clearly seen (white dovetail arrow in **D**) on MR image. CT fistulography (**A-C**) and MRI (contrast-enhanced liver acquisition with volume acceleration [LAVA] in **D, F**; T2-weighted with fat suppression in **E**): thick fistula (white arrow), minute fistula (white dovetail arrow), and long fistula (black dovetail arrow) are identified.

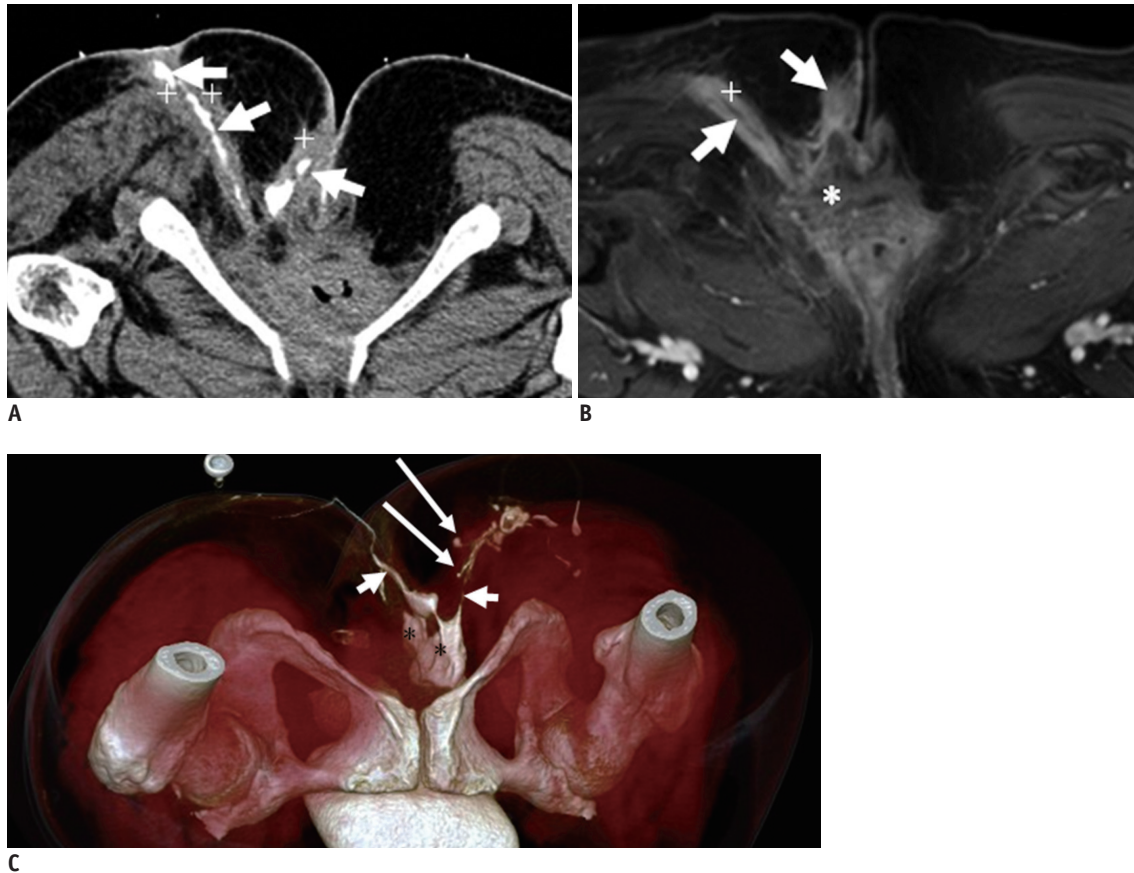


Fig. 4. 44-year-old female with recurrent fistulas after two operations.

CT fistulography (**A, C**) and MR imaging (contrast-enhanced T1-weighted with fat suppression in **B**): reconstructed images clearly show complicated spatial information of two separate fistula tracts (short white arrows) with irregularly shaped abscess (* in **C**), which closes to mid-anal canal. Internal tiny ramifications (long white arrows in **C**) are not exactly confirmed at corresponding position on MR image. Fistula cavities are surrounded by inflammatory tissue (fistula wall, + in **A, B**). Irregular shape of abscess (* in **B**).

the rectum and air was insufflated to the near maximum patient tolerance. Insufflation should be gradually performed and carefully monitored, using CT scout views, in order to avoid the risk of perforation. Patients should be informed that the distension may result in feeling of bloating.

An infusion tube with the needle removed was cut in at the site of external opening under the rigorous disinfection measures. The tip of the infusion tube was dipped in xylocaine gel for a local anesthetic effect and lubrication. The site of external opening was cleaned well with alcohol and a povidone-iodine solution. The infusion tube was cleaned thoroughly using a compatible enzymatic detergent. A prepared solution (1 mL gastrografin mixed in 10 mL of sterile normal saline) was gradually injected into the fistula. The volume of the contrast mixture was determined by the number of branches, width, and length of the perianal fistula, so different volumes of the contrast mixture were used in different patients. We determined

the optimal amount of contrast when reflow occurred from the external opening. We closed the external opening with sterile gauze when reflow occurred, and cleaned off any contrast refluxed on the skin's surface. We injected through all openings to fully fill the perianal fistula.

Advances in CT hardware and software enable scans to be performed with a much lower radiation dose than conventional CT scans. Sinogram-affirmed iterative reconstruction-enabled reconstruction provides abdominal CT images without a loss of diagnostic value at a 50% reduced dose and in some patients and at a 75% reduced dose in others (8). To obtain the best diagnostic image quality at the lowest possible radiation exposure, the following methods were adopted: 1) the tube current time product was set to 100 mAs over a scan length of 10 cm using combined modulation (50% lower dose, image reconstruction: iterative reconstruction); 2) scan range was confined to the smallest possible region to avoid direct radiation exposure of any unnecessary regions. The

Imaging of Anal Fistulas

images were reconstructed on a workstation, including the method of maximum intensity projection, multiple planar reconstruction, and volume rendering (VR).

Fistulography improves the diagnostic effectiveness in the

assessment of the fistulous course. However, fistulography is an invasive and painful procedure, requiring probing of the fistulous tract. An aggressive injection may injure tissues, cause false passages, and fail to demonstrate

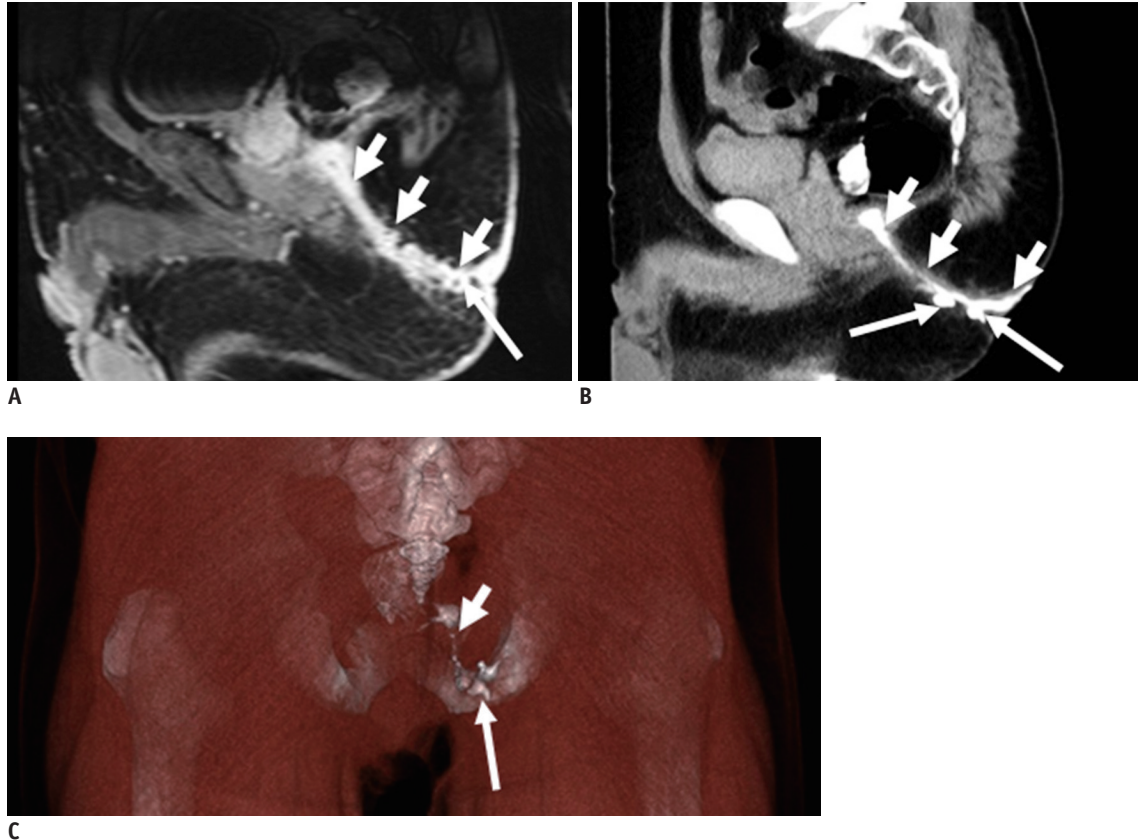


Fig. 5. 64-year-old male with perianal complex fistulas.

CT fistulography (**B, C**) and MR imaging (contrast-enhanced T1-weighted with fat suppression in **A**): reconstructed images clearly show complicated spatial information of fistula tract (short white arrows). Latent secondary extensions (long white arrows in **B, C**) are clearly confirmed on CT but not corresponding MR image (long white arrow in **A**).



Fig. 6. 64-year-old male with extrasphincteric fistula.

MR imaging (T2-weighted with fat suppression in **A**) and CT fistulography (**B**): internal opening (short white arrow in **A, B**) of fistula (+ in **A, B**) is well identified in corresponding MR and CT images; confirmation of internal opening is major surgical aim.

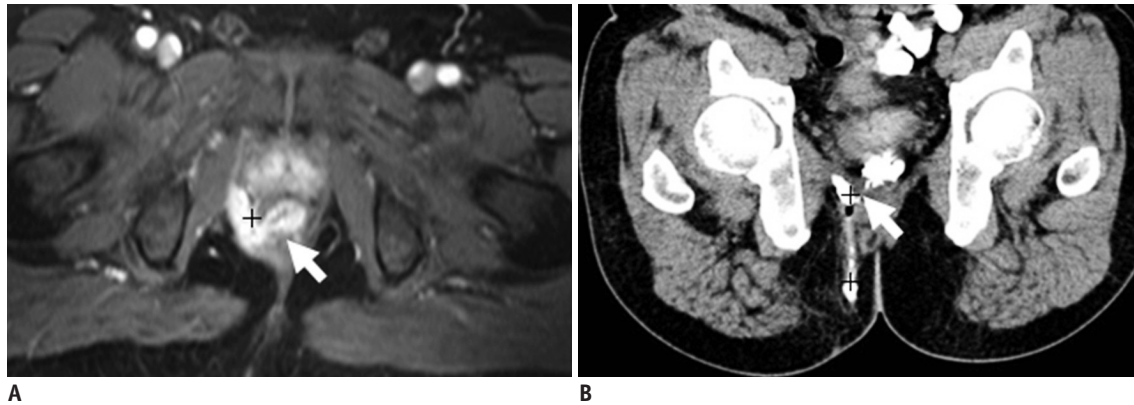


Fig. 7. 64-year-old male with perianal complex fistulas. MR imaging (contrast-enhanced T1-weighted with fat suppression in **A**) and CT fistulography (**B**): internal opening (short white arrow in **A, B**) of fistula (+ in **A, B**) is well identified in corresponding MR, CT images.

subtleties within the tract. It is also a time-consuming procedure that carries the risk of complications, including infection, sepsis, aggravation of pain, and others (9). Therefore, the reliability of the fistulography technique is related to a rigorous adherence to proper execution methods and to operator skill. In all of our cases, the procedures were performed by skilled surgeons who adhered to a strict aseptic technique in order to reduce pain and shorten the operation time. The initial contrast injection should be performed gently. However, in the presence of sepsis, fistulogram is contraindicated.

MR imaging of the pelvic cavity was first performed in all patients at our institution, but the detailed anatomical features of perirectal fistulae were still not well-seen in some special cases. As a result, CT fistulography had to be performed at the request of the clinicians.

Relevant Anatomy of the Perianal Region

The anal sphincter complex consists of two cylindrical layers separated by a fat-containing intersphincteric space (10). The understanding of fine perianal anatomical detail is crucial to provide an excellent road map prior to surgery. The anal sphincter complex with soft tissue density is seen on CT as two concentric rings separated by a sheet of fat, which appears to be of low density. The anal sphincter complex with hypointense imaging is seen on MRIs as two concentric rings separated by a sheet of fat appearing hyperintense (Figs. 1, 2).

Three-Dimensional Visualization

The acquisition of three-dimensional (3D) images is

necessary to increase precision in complicated fistula surgery. 3D T2-weighted turbo spin echo (TSE) sequences can serve as a source data set for the post-processing reconstruction of images from any desired plane (11). However, the 3D T2-weighted imaging protocol has limitations with regard to lesion conspicuity (12). T2-weighted MR imaging using 3D techniques has been used rarely because of the long acquisition times of the pulse sequences and their increased sensitivity to motion (13). To our knowledge, use of the 3D TSE sequence to image perianal fistulas has not been reported (11). Recently, volumetric thin-slice CT scanners have been found to be superior to MRIs in providing isotropic 3D datasets with a high resolution down to 0.4 mm³ (14). However, this method is often hindered by inadequate tissue contrast (15). The disadvantages of CT might be overcome by using CT fistulography, which offers the possibility of isotropic voxels and high contrast (16). In this review, the 3D visualization of perianal fistulas was perfectly obtained from any arbitrary viewing point in CT workstation (Fig. 3). A grasp of the solid positional relation between the perianal fistulas and the perianal soft tissue is important. It improves the surgeon's knowledge of the perianal fistulas' anatomy, aiding in pre-surgical prediction. During the 3D planning process, the surgeon simulates the operation and defines the position and geometry of the perianal fistulas. Programming of the incision line may be not easy when based on MR imaging only, although all the information is there. By using such fistulas/perianal soft tissue 3D-reconstructed CT images, operation simulation becomes easier and less time-consuming.

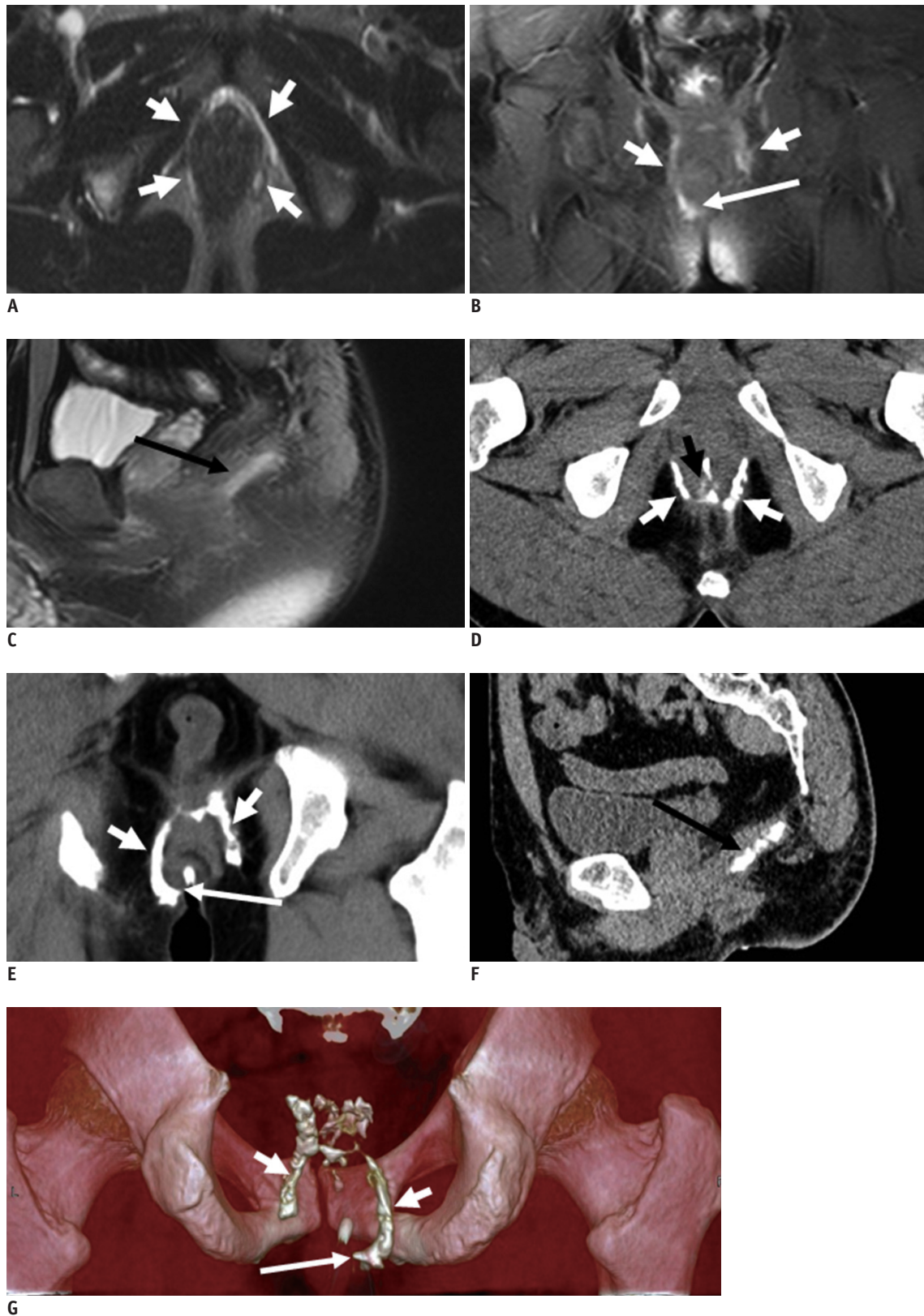


Fig. 8. 38-year-old male with semi-horseshoe fistula.

CT fistulography (D-G) and MR imaging (T2-weighted with fat suppression in A-C): transverse, coronal images clearly show circumferential spread of fistula (short white arrows in A-G). Extent of disease and complicated spatial information are better seen on volume rendering image (short arrows in G). External opening (long white arrow in B, E, G), internal opening (short black arrow in D), and secondary ramification (long black arrow in C, F) are seen.

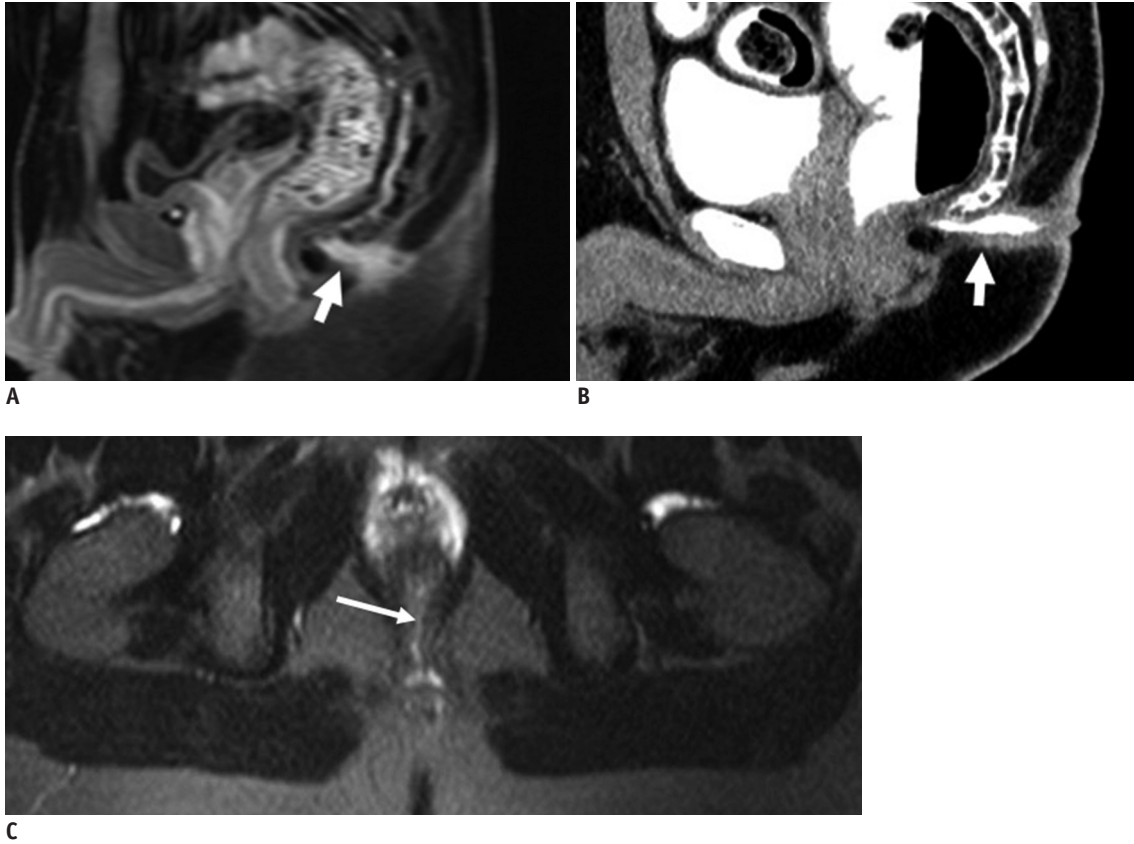


Fig. 9. 26-year-old male with fistula.

MR imaging (T1-weighted with fat suppression in **A**, T2-weighted with fat suppression in **C**) and CT fistulography (**B**): fistula (short white arrow in **A**, **B**) spreads backward to skin's surface with evident external opening. Tenuous internal opening (long white arrow in **C**) was successfully identified on MR image. Internal opening is confirmed clearly on MR image but not corresponding CT image, owing to lack of contrast agent filling.

Extension of the Primary Fistulous Track and the Affected Pelvic Structures

The major advantage of MR imaging is its capacity to demonstrate extensions associated with a primary tract. Morphologically, MRI's ability to accurately demonstrate the fistula's extensions may provide an excellent road map prior to surgery. When the primary fistulous track was identified on CT fistulography images in our review, several imaging features require assessment in order to perform an accurate preoperative assessment: the length of fistulous track, the number of ramifications, thickening of the fistulous wall, and the area of the affected pelvic structures. An important advantage of CT imaging in fistula evaluation is that inflammatory streaking can be clearly displayed by the backdrop of extremely low-density fat in the ischioanal fossa (17). To some extent, contrast-enhanced CT images contribute to the evaluation of granulation tissue and its relationship to the sphincter.

Internal Opening, External Opening, and Latent Ramifications

Preoperative CT fistulography is well-suited to the identification of the internal and external openings and latent ramifications, especially for tiny lesions. More importantly, an internal opening in continuity with one or more external openings can be displayed with a 3D effect by the VR technique. In addition, latent ramifications are often too hidden for easy identification due to the relatively thick slices or complex signals in MR imaging (Figs. 4-8). The major disadvantage of CT fistulography is that the secondary ramification or the primary tract may fail to fill with contrast material if plugged with debris, and in particular, the technique depends primarily on the existence of an external opening. In our studies, we were unable to inject contrast agent into the fistula in ano via the external opening in 8.3% of cases (2 of 24 patients), and the internal opening was not confirmed owing to the lack of contrast agent filling in 20.7% of cases (5 of 24 patients).



Fig. 10. 25-year-old female with fistula.

MR imaging (T2-weighted with fat suppression in **A**, contrast-enhanced liver acquisition with volume acceleration in **C**) and CT fistulography (**B**). Fistula (short white arrows in **C**) perforating backward toward anal sphincter, spreads (short white arrow in **A**) backward to skin's surface with evident external opening (long white arrow in **A**, **B**). Fistula is confirmed clearly on MR image but not corresponding CT image, owing to lack of contrast agent filling.

When the opening fails to fill with the contrast material, MR imaging may be the best choice to visualize the internal opening (Figs. 9, 10).

Classification of Perianal Fistulas

The anatomic description of the perianal fistulas and the location of any associated extension form its "classification". Fistulas may be accordingly classified as intersphincteric, transsphincteric, suprasphincteric, and extrasphincteric sections (18). The description of perianal fistulas in a radiology report should include an identification of the primary track and its orientation with reference to the anal sphincter complex. To avoiding the disability of anal continence in a sphincter-interrupting procedure, a detailed preoperative definition regarding the classification of perianal fistulas is of great importance. The information obtained with MR imaging appears to be a more powerful predictor of postoperative outcome than the information gained from surgical exploration (19, 20). In this review,

CT fistulography also provided a precise definition of the fistulous track, along with its relationship to pelvic structures (Figs. 6, 7).

Deep Pelvic Abscess or Mass with Secondary Fistula

Deep pelvic abscess or necrotic pelvic mass with secondary fistula may present a unique challenge for percutaneous drainage because of numerous overlying structures, precluding safe percutaneous access (21). In MR imaging, an abscess that contains air may be difficult to visualize or differentiate from air in the adjacent bowel. On the contrary, the CT is free from these limitations. CT provides 3D imagery of the internal organs and abnormal growth in the deep area, thus aiding the physician in detecting the specific location of any pathological changes (Fig. 11).

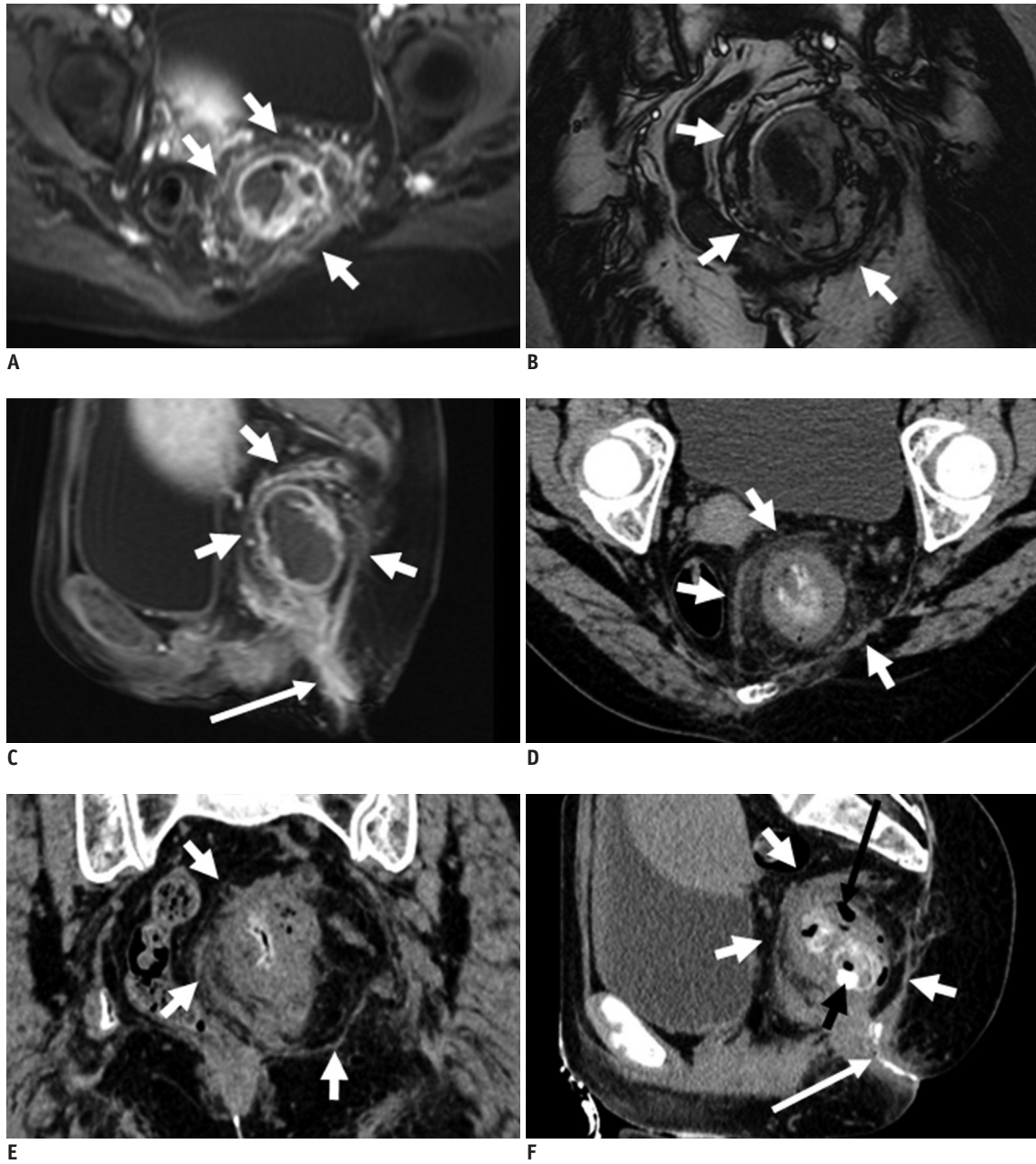


Fig. 11. 54-year-old female with fistula caused by ruptured teratoma in pelvic cavity.

MR imaging (contrast enhanced T1-weighted with fat suppression in **A, C**; T2-weighted without fat suppression image in **B**), and CT fistulography (**D-F**): mass (teratoma, short white arrows in **A-F**) perforates levator ani muscle downward, entering perianal spaces. Images (**A-F**) provide excellent imaging of fistula (long white arrow in **C, F**), teratoma, and their relationship to adjacent organ organization. Calcification (short black arrow in **F**) and gas (long black arrow in **F**) in teratoma can be seen.

CONCLUSIONS

In summary, CT fistulography and MR imaging have their respective advantages for the preoperative evaluation of perianal fistulas and can be applied in a complementing manner when necessary. The organic combination of these two modalities may improve the surgeon's knowledge regarding the morphology of the fistulas, making even more

complicated surgery on complex fistulas safer.

REFERENCES

1. Seow-Choen F, Nicholls RJ. Anal fistula. *Br J Surg* 1992;79:197-205
2. Practice parameters for treatment of fistula-in-ano--supporting documentation. The Standards Practice Task Force.

- The American Society of Colon and Rectal Surgeons. *Dis Colon Rectum* 1996;39:1363-1372
3. Lilius HG. Fistula-in-ano, an investigation of human foetal anal ducts and intramuscular glands and a clinical study of 150 patients. *Acta Chir Scand Suppl* 1968;383:7-88
 4. Seow-Choen, Phillips RK. Insights gained from the management of problematical anal fistulae at St. Mark's Hospital, 1984-88. *Br J Surg* 1991;78:539-541
 5. Bartram C, Buchanan G. Imaging anal fistula. *Radiol Clin North Am* 2003;41:443-457
 6. de Miguel Criado J, del Salto LG, Rivas PF, del Hoyo LF, Velasco LG, de las Vacas MI, et al. MR imaging evaluation of perianal fistulas: spectrum of imaging features. *Radiographics* 2012;32:175-194
 7. Yousem DM, Fishman EK, Jones B. Crohn disease: perirectal and perianal findings at CT. *Radiology* 1988;167:331-334
 8. Kalra MK, Woisetschläger M, Dahlström N, Singh S, Lindblom M, Choy G, et al. Radiation dose reduction with Sinogram Affirmed Iterative Reconstruction technique for abdominal computed tomography. *J Comput Assist Tomogr* 2012;36:339-346
 9. Tio TL, Mulder CJ, Wijers OB, Sars PR, Tytgat GN. Endosonography of peri-anal and peri-colorectal fistula and/or abscess in Crohn's disease. *Gastrointest Endosc* 1990;36:331-336
 10. Lunniss PJ, Phillips RK. Anatomy and function of the anal longitudinal muscle. *Br J Surg* 1992;79:882-884
 11. Proscia N, Jaffe TA, Neville AM, Wang CL, Dale BM, Merkle EM. MRI of the pelvis in women: 3D versus 2D T2-weighted technique. *AJR Am J Roentgenol* 2010;195:254-259
 12. Kim H, Lim JS, Choi JY, Park J, Chung YE, Kim MJ, et al. Rectal cancer: comparison of accuracy of local-regional staging with two- and three-dimensional preoperative 3-T MR imaging. *Radiology* 2010;254:485-492
 13. Fütterer JJ, Yakar D, Strijk SP, Barentsz JO. Preoperative 3T MR imaging of rectal cancer: local staging accuracy using a two-dimensional and three-dimensional T2-weighted turbo spin echo sequence. *Eur J Radiol* 2008;65:66-71
 14. Flohr T, Stierstorfer K, Raupach R, Ulzheimer S, Bruder H. Performance evaluation of a 64-slice CT system with z-flying focal spot. *Rofo* 2004;176:1803-1810
 15. Lichy MP, Wietek BM, Mugler JP 3rd, Horger W, Menzel MI, Anastasiadis A, et al. Magnetic resonance imaging of the body trunk using a single-slab, 3-dimensional, T2-weighted turbo-spin-echo sequence with high sampling efficiency (SPACE) for high spatial resolution imaging: initial clinical experiences. *Invest Radiol* 2005;40:754-760
 16. Halligan S, Stoker J. Imaging of fistula in ano. *Radiology* 2006;239:18-33
 17. Liang C, Jiang W, Zhao B, Zhang Y, Du Y, Lu Y. CT imaging with fistulography for perianal fistula: does it really help the surgeon? *Clin Imaging* 2013;37:1069-1076
 18. Parks AG, Gordon PH, Hardcastle JD. A classification of fistula-in-ano. *Br J Surg* 1976;63:1-12
 19. Spencer JA, Chapple K, Wilson D, Ward J, Windsor AC, Ambrose NS. Outcome after surgery for perianal fistula: predictive value of MR imaging. *AJR Am J Roentgenol* 1998;171:403-406
 20. Chapple KS, Spencer JA, Windsor AC, Wilson D, Ward J, Ambrose NS. Prognostic value of magnetic resonance imaging in the management of fistula-in-ano. *Dis Colon Rectum* 2000;43:511-516
 21. Harisinghani MG, Gervais DA, Hahn PF, Cho CH, Jhaveri K, Varghese J, et al. CT-guided transgluteal drainage of deep pelvic abscesses: indications, technique, procedure-related complications, and clinical outcome. *Radiographics* 2002;22:1353-1367